Distinct calcium/calmodulin-dependent serine protein kinase domains control cardiac sodium channel membrane expression and focal adhesion anchoring

Adeline Beuriot, Catherine A Eichel, Gilles Dilanian, Florent Louault, Dario Melgari, Nicolas Doisne, Alain Coulombe, Stéphane N. Hatem, Elise Balse

JHRM-D-19-01432

Distinct Calcium/CAlmodulin-dependent Serine protein Kinase domains control cardiac sodium channel membrane expression and focal adhesion anchoring

Running title: Structure-function of CASK in cardiomyocyte

Adeline Beuriot, PhD[1], Catherine A. Eichel, PhD[1], Gilles Dilanian, MSc[1], Florent Louault, MSc[1], Dario Melgari, PhD[1], Nicolas Doisne, PhD[1], Alain Coulombe, PhD[1], Stéphane N. Hatem, MD, PhD[1,2] and Elise Balse, PhD[1*]

[1]INSERM UMRS1166, ICAN - Institute of CardioMetabolism and Nutrition, Sorbonne Université, Paris, France
[2]Institut de Cardiologie, Hôpital Pitié-Salpêtrière, Paris, France

*Corresponding author:
Dr. Elise Balse, PhD
INSERM UMRS1166
Faculté de Médecine Pitié-Salpêtrière
91, Boulevard de l'Hôpital
75013 Paris
E-mail: elise.balse@upmc.fr

ORCID: https://orcid.org/0000-0001-5224-9180

Conflict of interest statement:
The authors declare no conflict of interests.

Word count: 4959

ABSTRACT:

Background: Membrane-associated guanylate kinase (MAGUK) proteins function as adaptor proteins to mediate the recruitment and scaffolding of ion channels in the plasma membrane in various cell types. In the heart, the protein CASK (Calcium/CAlmodulin-dependent Serine protein Kinase) negatively regulates the main cardiac sodium channel, $Na_V1.5$, which carries the sodium current (I_{Na}) by preventing its anterograde trafficking. CASK is also a new member of the dystrophin-glycoprotein complex, and like syntrophin, binds to the C-terminal domain of the channel.
Objective: To unravel the mechanisms of CASK-mediated negative I_{Na} regulation, and interaction with the dystrophin-glycoprotein complex in cardiac myocytes.
Methods: CASK adenoviral truncated constructs with sequential single functional domain deletions were designed for overexpression in cardiac myocytes: $CASK^{\Delta CAMKII}$, $CASK^{\Delta L27A}$, $CASK^{\Delta L27B}$, $CASK^{\Delta PDZ}$, $CASK^{\Delta SH3}$, $CASK^{\Delta HOOK}$, and $CASK^{\Delta GUK}$. Combination of whole-cell patch-clamp recording, total internal reflection fluorescence microscopy (TIRFm) and biochemistry experiments were conducted in cardiac myocytes to study the functional consequences of domain deletions.
Results: We show that both L27B and GUK domains are required for the negative regulatory effect of CASK on I_{Na} and $Na_V1.5$ surface expression and that the HOOK domain is essential for interaction with the cell adhesion dystrophin-glycoprotein complex.
Conclusions: This study demonstrates that the multi-modular structure of CASK confers an ability to simultaneously interact with several targets within cardiomyocytes. Through its L27B, GUK, and HOOK domains, CASK potentially provides the ability to control channel delivery at adhesion points in cardiomyocyte.

230 words

Keywords: MAGUK, CASK, sodium channel, dystrophin, cardiomyocyte

INTRODUCTION

The nature of mechanisms regulating the delivery of newly addressed ion channels and their subsequent organization in the plasma membrane remains to be addressed in cardiomyocyte. Interestingly, members of the Membrane-Associated GUanylate Kinase homologs (MAGUK proteins), a family of multi-domain membrane proteins, have emerged as central organizers of specialized plasma membrane domains in various cell types including cardiomyocytes. MAGUK proteins are able to interact with transmembrane proteins such as ion channels and receptors as well as with cytoplasmic proteins including scaffold, cytoskeleton and trafficking proteins, molecular motors, and signaling enzymes[1]. As such, MAGUK proteins have crucial roles in organization of cellular polarity, cell-cell adhesion, and dynamic regulation of large macromolecular complexes[2].

MAGUK proteins display basic core structure comprising three canonical protein-protein interacting domains: PDZ, SH3, and GUK. The MAGUK protein CASK (calcium/calmodulin-dependent serine protein kinase) comprises three additional domains serving as protein-protein interaction modules: a N-terminal CAMKII domain, a pair of L27 domains, and a HOOK domain preceding the C-terminal GUK domain. In polarized cells, the role of each functional domain of CASK has been extensively investigated. The CAMKII domain interacts with Mint1 and liprin-α, both involved in vesicle exocytosis in presynaptic terminals[3,4]. The L27A domain targets the MAGUK SAP97 at the basolateral membrane in epithelial cells[5]. The association of L27B to the multi-adaptator protein Veli drives the basolateral distribution of Kir2.3 channels (Alewine et al., 2007). The PDZ domain recognizes C-terminal sequences on transmembrane and cytoplasmic target proteins. The SH3 domain binds GUK domains, enabling formation of CASK dimers[6] and proline-rich motifs on target proteins, such as the C-terminal domain of calcium channel. This interaction involves Mint1 and helps channel trafficking to the membrane and subsequent delivery of new cargo vesicles through Ca^{2+} influx[7]. The HOOK domain interacts with the cytoskeleton protein 4.1 and with adhesion molecules such as neurexin and syndecan-2[8,9]. The GUK domain interacts with transcription factors[10–12] and mediates the interaction between the presynaptic protein rabphilin3a and neurexin[13].

We previously reported that, in contrast to other partners of the main cardiac sodium channel, $Na_V1.5$, CASK regulates the sodium current in a negative way in cardiomyocyte. We showed that CASK impedes anterograde trafficking of $Na_V1.5$ channel and associates with the costameric dystrophin-syntrophin complex[14]. Here we investigated the role of the different CASK domains in regulating the $Na_V1.5$/dystrophin-glycoprotein macromolecular complex using CASK adenoviral constructs with sequential functional domain deletion. Using a combination of whole-cell patch-clamp, total internal reflection fluorescence (TIRF) microscopy and biochemistry, we showed that L27B and GUK domains are involved in CASK negative regulatory effect on I_{Na} and $Na_V1.5$ surface expression in cardiomyocytes whereas the HOOK domain is responsible for interactions with the dystrophin-glycoprotein complex. This study provides new insights into how the multi-modular structure of CASK makes the link between $Na_V1.5$ functional expression at the membrane and focal adhesion sites related to the dystrophin-glycoprotein complex in cardiomyocyte.

RESULTS

Design and expression of truncated CASK adenoviral constructs in cardiomyocytes. We designed one full-length CASK protein corresponding to the 100 kDa cardiac isoform ($CASK^{WT}$) and seven domain-specific deletion versions in which one single domain was truncated at a time ($CASK^{\Delta X}$). Deleted CASK proteins and full-length CASK were fused to a C-terminal GFP reporter (Figure 1A). GFP alone serves as a control condition. All constructs were sub-cloned into adenoviral vectors to enable overexpression in adult rat cardiomyocytes. Figure 1A shows the expected molecular weights of the various CASK isoforms. Western blot

experiments performed on lysates obtained from cultured ventricular adult rat cardiomyocytes three days after adenoviral transduction confirmed CASK protein overexpression at anticipated molecular weights (Figure 1B). A range of 100 to 140 kDa proteins corresponding to the full-length protein or truncated forms of CASK plus GFP was observed at significantly higher levels for $CASK^{WT}$ and $CASK^{\Delta X}$ than the GFP control expressing only endogenous CASK (Figure 1B). RT-qPCR experiments performed on total mRNA isolated from cardiomyocytes three days after adenoviral infections demonstrated an average 6-fold increase in CASK mRNA levels for all eight constructs compared to the GFP control. Both $CASK^{WT}$ and $CASK^{\Delta X}$ constructs had equivalent mRNA expression levels, supporting that all constructs had similar transduction efficacy in cardiomyocytes (Figure 1C).

Characterization of CASK domains involved in sodium current regulation and $Na_V1.5$ surface expression in cardiomyocytes.

We previously showed that CASK acts as a negative regulatory partner of the cardiac sodium current I_{Na} by preventing anterograde trafficking and surface expression of $Na_V1.5$ channels in the sarcolemma[14]. Here, we investigated the role of the different CASK domains in I_{Na} regulation and $Na_V1.5$ surface expression.

First, whole-cell patch-clamp experiments were conducted in adult rat cardiomyocytes three days after transduction. For all constructs, i.e. $CASK^{WT}$ and $CASK^{\Delta X}$, sodium current density was compared to GFP control, expressing endogenous CASK only. I_{Na} was reduced by ~50% in $CASK^{WT}$-transduced cardiomyocytes ($P<0.001$). Similarly, average current-voltage (I-V) plots from voltage clamp experiments showed significant decreases in I_{Na} densities at different tested voltages in $CASK^{\Delta CAMKII}$, $CASK^{\Delta L27A}$, $CASK^{\Delta PDZ}$, $CASK^{\Delta SH3}$, and $CASK^{\Delta HOOK}$-transduced cardiomyocytes ($P<0.001$). On the contrary, deletion of either L27B or GUK domains prevented the reduction of I_{Na}, and both $CASK^{\Delta L27B}$ and $CASK^{\Delta GUK}$ showed similar current densities to GFP control-transduced cardiomyocytes (Figure 2A-B). Cell capacitances were similar between the different conditions, implying that CASK does not significantly influence cell growth. Activation or steady-state inactivation properties were not changed between GFP, $CASK^{WT}$, and $CASK^{\Delta X}$ (Figure 2C-D; Supplemental Table 1). These experiments demonstrate that CASK's I_{Na} inhibiting function is dependent on functional L27B and GUK domains.

Second, total internal reflection fluorescence microscopy (TIRFm) was used to quantify the evanescent field fluorescence (EFF) intensity of the $Na_V1.5$ signal in the membrane plane. Three days after transduction, cardiomyocytes seeded on TIRF-glass micro-dishes were fixed and stained with anti-$Na_V1.5$ antibody. Cell boundaries were delineated using differential interference contrast (DIC) images and $Na_V1.5$ EFF was quantified in critical angle in GFP control, $CASK^{WT}$, $CASK^{\Delta L27B}$, and $CASK^{\Delta GUK}$ (Figure 3A). TIRF experiments showed a ~30% decrease in $Na_V1.5$ surface staining in $CASK^{WT}$ cardiomyocytes compared to GFP control ($P<0.001$) (Figure 3B). In contrast, the $Na_V1.5$ EFF signal in either $CASK^{\Delta L27B}$- or $CASK^{\Delta GUK}$-transduced myocytes was of similar intensity to that measured in GFP control (Figure 3B).

Third, RT-qPCR and Western blot experiments showed no changes in *scn5a* copy number and in global $Na_V1.5$ protein expression between GFP control, $CASK^{WT}$, and $CASK^{\Delta X}$ (Supplemental Figure 1), excluding the involvement of CASK in translational regulation of *SCN5A* gene encoding $Na_V1.5$ channel.

Characterization of the CASK domain interacting with dystrophin in cardiomyocytes.

Using immunocytochemistry and co-immunoprecipitation assays, we previously showed that CASK associates with dystrophin at the lateral membrane of cardiomyocytes. Immunostaining performed on dystrophin-deficient mdx mouse ventricular cryosections showed a loss of CASK staining, suggesting that CASK expression at the lateral membrane depends on dystrophin expression[14]. Here, we investigated whether a specific CASK domain was involved in the interaction between CASK and dystrophin.

Western blot experiments showed that $CASK^{WT}$ or $CASK^{\Delta X}$ overexpression did not modify dystrophin expression levels compared to GFP control (Figure 4A-B). The association

between CASK and dystrophin was again supported by co-immunoprecipitation experiments performed on cardiomyocyte lysates overexpressing $CASK^{WT}$ (Figure 4C). Dystrophin was able to precipitate CASK with all truncated $CASK^{\Delta X}$ constructs except for $CASK^{\Delta HOOK}$ (Figure 4C). These results suggest that the ~10 amino acids HOOK domain of CASK is responsible for interactions with the costameric dystrophin-glycoprotein complex in cardiomyocytes. The fact that $CASK^{\Delta HOOK}$ does not rescue I_{Na} suggests that the HOOK domain is not involved in channel trafficking, but instead likely involved in organizing focal adhesions, notably costameric complexes in cardiomyocyte.

DISCUSSION

We previously characterized CASK as an unconventional partner of Nav1.5 channel. In particular, we described CASK negative regulatory function on the sodium channel anterograde trafficking and its restricted localization in the dystrophin-glycoprotein complex of cardiomyocytes. Here, using multidisciplinary approaches including adenoviral constructs with sequential functional domain deletion, we showed that CASK carries out its regulation of Nav1.5 channel anterograde trafficking through L27B and HOOK domains. Moreover, the interaction between CASK and the dystrophin-glycoprotein complex is achieved through the HOOK domain. To the best of our knowledge, this study is the first to identify a sodium channel partner with the potential to control ion channels delivery to adhesion points in cardiomyocytes.

L27B and GUK domains regulate sodium current and $Na_V1.5$ surface expression in cardiomyocyte.

Our findings that both L27B and GUK domains of CASK regulates $Na_V1.5$ channel functional expression at the membrane are particularly interesting considering the known functions of these two domains in neurons. In the pre-synaptic terminal, CASK binds both Mint1 and Veli, respectively through CAMKII and L27B domains[3,15]. Due to its interactions with both neurexin and vesicular trafficking-related proteins, the Mint1/Veli/CASK complex has been proposed to couple synaptic vesicle exocytosis to neuronal cell adhesion. In this line, the Mint1/Veli/CASK complex also participates in anterograde trafficking of glutamate receptors along microtubules by bridging to KIF-17[16]. Differential sorting of glutamate receptor subtypes has also been shown to depend on additional protein associations with the Mint1/Veli/CASK, notably SAP97[17,18]. Other studies also reported interactions between the GUK domain of CASK and rabphilin-3a, suggesting that the rabphilin-3a/CASK/neurexin complex could participate in the guidance of presynaptic vesicles towards exocytosis zones[13].

Consistent with these observations, the existence of distinct $Na_V1.5$ channel subpopulations has been proposed in cardiomyocyte relying on association with specific partners and specific localization in the sarcolemma. $Na_V1.5$ channels are highly concentrated at the intercalated disc where they associate with gap junctional, desmosomal, actin cytoskeleton-binding, and MAGUK proteins. $Na_V1.5$ channels at the lateral membrane show a lower density and interact with syntrophin and CASK[19]. The consequence of this differential distribution is to favor anisotropic (longitudinal>transversal) propagation of the action potential in the myocardium. Despite the regulatory function of these partners on the sodium current is clearly established, their role in trafficking, scaffolding and/or stabilization has not been investigated, except for CASK which prevent early trafficking of the channel[14]. Although the precise location of $Na_V1.5$ in membrane subdomains has not been investigated here, our data demonstrates that both L27B and GUK domains are mandatory in regulating the functional expression of $Na_V1.5$ channel in cardiomyocyte sarcolemma. Considering the functions of L27B and GUK domains in neurons, one could speculate that interaction with specific partner(s) and/or competition between partners at early stages of trafficking could determine the sorting and final targeting of the channel in cardiomyocytes.

Role of the CASK HOOK domain in scaffolding of macromolecular complex.

We previously showed that CASK is enriched in dystrophin-glycoprotein complexes, a costameric complex located at cardiomyocyte lateral membranes[14]. Costameres function as

focal adhesions in other cell types. They constitute physical links between sarcomeric z-lines, the sarcolemma, and the extracellular matrix and guarantee the three-dimensional organization of the myocardium when sheets of myocytes slide against each other during each contraction. Here we show that CASK interacts with dystrophin through its HOOK domain.

The HOOK domain of CASK corresponds to a protein 4.1 binding motif[21]. By binding spectrin and cytoskeletal actin, protein 4.1 plays critical role in membrane mechanical stability[22]. In epithelial cells, transmembrane syndecan is anchored to actin cytoskeleton though interactions between CASK and protein 4.1[23]. In the synapse, neurexin and neuroligin are connected to cytoskeletal actin through CASK and protein 4.1 interactions[8]. A large macromolecular complex formed of CASK, neurexin, Mint1, Veli, protein 4.1, spectrin, and actin, organizes and stabilizes the presynaptic element[8]. in heart and skeletal muscle cells, the Mint1/Veli/SAP97/CASK complex was also found to be associated with ion channels, notably Kir2.x channels. Kir2.x channels also interact with components of the dystrophin-glycoprotein complex including syntrophin, dystrophin, and dystrobrevin at the neuromuscular junction, although with lower affinities[24]. In this line, using GST pull-down experiments we previously showed a direct interaction between purified CASK protein and the $Na_V1.5$ C-terminal[14]. Interestingly, the same $Na_V1.5$ channel C-terminal domain also interact (directly or indirectly) with syntrophin[25]. The fact that CASK and syntrophin exert opposite effects on the sodium current suggest a possible competition between the two partners. As CASK prevents anterograde trafficking of sodium channel at early stage of trafficking, the question of $Na_V1.5$ channel sorting by its partners remains to be investigated.

Here, the fact that $CASK^{\Delta HOOK}$ does not rescue I_{Na} suggests that the HOOK domain is not involved in channel trafficking, but instead likely involved in organizing costameric complexes. Interestingly, CASK expression is reduced in remodeled myocardium in both rat and human[14], suggesting that changes in working conditions of the heart could affect costameric organization and consequently impact $Na_V1.5$ channel exocytosis in cardiomyocyte.

CONCLUSION

Mounting evidence indicates that distinct populations of $Na_V1.5$ channels exist in cardiomyocytes. These populations reside in different membrane sub-domains and depend on the channels association with specific regulatory partners. Although the exact location of $Na_V1.5$ different sub-populations within the membrane was not the primary objective of this study, we provided new insights into the mechanisms that potentially allow the multi-modular structure of CASK to control $Na_V1.5$ channel delivery at adhesion points in cardiomyocytes. Nevertheless, the question of how $Na_V1.5$ channels are dynamically and specifically targeted to distinct membrane domains is still to be addressed. Therefore, in order to follow the channel sorting and final targeting, the real-time investigation of the association and co-trafficking of $Na_V1.5$ with its different partners will be warranted. Such studies should contribute to a better understanding of how specific targeting of $Na_V1.5$ channel into cardiomyocyte is dynamically achieved to ensures cardiac anisotropy and contribute to sodium channel-related arrhythmias.

MATERIAL and METHODS

Animals

Studies were performed in adult male Wistar rats (~200 g, Janvier Labs, France). All animals were treated in accordance with French Institutional guidelines (Ministère de l'Agriculture, France, authorization 75-1090) and conformed to the Directive 2010/63/EU of the European Parliament for the use and care of animals.

Isolation and culture of adult rat cardiomyocytes

Adult atrial or ventricular cardiomyocytes were obtained by enzymatic dissociation on a Langendorff column as previously described[14]. Briefly, rats were anesthetized with an i.p.

injection of pentobarbital sodium (110 mg/kg) and heparin sodium (250 units/kg). The heart was then excised and cannulated via the aorta on a Langendorff apparatus and perfused in a constant flow rate (5mL/min). The perfusate consisted as an enzymatic solution containing in mmol/L: NaCl 100, KCl 4, MgCl2 1.7, glucose 10, $NaHCO_3$ 5.5, KH_2PO_4 1, HEPES 22, BDM 15 and 200UI/mL collagenase A (Roche Diagnostics) plus bovine serum albumin 7.5, pH 7.4 (NaOH) for ~20 min. Solution was equilibrate with 95% O2 and 5% CO_2 and maintained at a temperature of 37°C. Atrial and ventricular tissues were separated and cut into small pieces and cells were gently dissociated with pipettes in Kraft-Brühe (KB) solution, in mmol/L: glutamate acid potassium salt monohydrate 70, KCl 25, taurine 20, KH_2PO_4 10, $MgCl_2$ 3, EGTA 0.5, glucose 10, and HEPES 10. Cardiomyocytes were plated on Petri dishes or Ibidi micro-dishes double-coated with Poly-D-lysine/laminin (Roche/Sigma). Cells were maintained under standard conditions (37°C, 5% CO2) in M199 medium (Gibco) supplemented with 1% penicillin/streptomycin (Gibco), 5% fetal bovine serum (Gibco) and 1‰ insulin/transferrin/selenium cocktail (Sigma). Isolated cells were used for immunofluorescence, biochemistry experiments or patch-clamp recordings after 3days in culture.

Adenoviruses

Full-length CASK ($CASK^{WT}$) and truncated sequences ($CASK^{\Delta CAMKII}$, $CASK^{\Delta L27A}$, $CASK^{\Delta L27B}$, $CASK^{\Delta PDZ}$, $CASK^{\Delta SH3}$, $CASK^{\Delta HOOK}$, $CASK^{\Delta GUK}$) were designed and cloned into a pShuttle vector with CMV promotor. Expression cassettes were transferred into the adenovirus vector containing GFP reporter for selection of infected cells. All the production, amplification and purification process were conducted by a Vector Production Center (Gene Therapy Laboratory, INSERM U1089, IRT-1, Nantes, France). Rat adult cardiomyocytes were transduced 24h after isolation with 5.10^7 particles/ml of $CASK^{WT}$, $CASK^{\Delta X}$ or empty vector (GFP) as negative control only expressing endogenous CASK. Overexpression studies were performed 3 days post-transduction.

Immunofluorescence and deconvolution microscopy

Cells fixation was performed with paraformaldehyde 4% (Sigma) for 10 min at room temperature (RT). For permeabilization, cells were incubated in PBS supplemented with 0.1% Triton X-100, 1% BSA, 10% sera for 1h at RT. Primary antibodies were applied over night at 4°C with blocking buffer (PBS containing 1% BSA, 3% sera, diluted antibodies according to the manufacturer's instructions. Secondary antibodies (2.5 to 5 µg/mL) FITC (Abcam) or AlexaFluor594 (Life Technologies) and DAPI (0.2µg/µL Sigma) to detect nuclei were diluted in blocking buffer and added on samples for 1h incubation at RT.

Total Internal Reflection Fluorescence microscopy (TIRFm)

Fluorescence intensity at surface membrane was visualized using the Olympus $Cell^{tirf}$ system. Cells were placed on an Olympus IX81-ZDC2 inverted microscope and TIRF illumination was achieved with the motorized integrated TIRF illuminator combiner (MITICO-2L) and dual band optical filter (M2TIR488-561) using a 60X/1.49 APON OTIRF oil immersion objective, allowing GFP and RFP visualization. All image acquisitions, TIRF angle adjustment and some of the analysis were performed using the xcellence software (Olympus). Fluorescence analysis was performed using ImageJ software (NIH).

Protein extraction

Cardiomyocytes expressing the appropriate constructs were lysed by scraping the cells into a lysis buffer, in mmol/L: Tris 50 (pH 7.5), NaCl 150, EDTA 2, 1% Triton X-100 and 1 ‰ protease cocktail inhibitor (Sigma Aldrich) and lysates were placed on a rotating 3D shaker for 1h at 4°C. After centrifugation, protein concentrations per supernatant were then determined by the BCA method (Pierce).

Co-Immunoprecipitation assays

Cardiomyocytes were lysed as described above. Lysates were then incubated all night with antibodies (10µg) or IgG mouse (0.1µg/mL) at 4°C on a rotating 3D shaker. G-Sepharose

beads (50µL for 2mg of total proteins, Sigma) were added for 1h before being washed with lysis buffer 3 times. Protein complexes bound to washed-beads were eluted with 2X sample buffer, followed by a denaturation step before separation by western blot.

Western Blot analysis

NuPAGE® Novex® 10 % Bis-Tris or 3-8 % Tris acetate gels (Life Technologies) were used, depending on the size of expected proteins. Proteins were transferred onto nitrocellulose membrane (Biorad) and blocked with 5% nonfat dry milk for 60 min and probed overnight at 4°C with primary antibodies. Anti-rabbit or anti-mouse horseradish peroxidase-conjugated secondary antibodies (Cell Signaling) were used before revealing membrane with a chemiluminescent detection reagent ECL Prime (GE Healthcare). Images were acquired using a ImageQuant LAS4000 camera system (GE Healthcare) and then analyzed with the ImageJ software. The relevant spots were measured and normalized versus that of the corresponding spot in the control condition. These normalized densities were averaged from at least 3 independent experiments.

Antibodies

Polyclonal rabbit antibody recognizing $Na_V1.5$ was obtained from Alomone Labs (ASC-005, 8µg/mL). Monoclonal mouse anti-CASK used for biochemical assays were form Origene (Clone S56A-50, TA326522, 1.5-5µg/mL) and Merck Millipore (Clone 2G5.1, MABN1547, 0.6µg/mL). Monoclonal rabbit anti-GAPDH was purchased from Cell Signaling (Clone 14C10, 2118, 1:40000). Polyclonal rabbit anti-GFP used for immunochemistry (0.3µg/mL) and western blotting (2µg/mL) was obtained from CliniSciences (TP401). Monoclonal mouse anti-Dystrophin (Clone MANDYS8, D8168, 0.6µg/mL) used for biochemical assays were purchased from Sigma.

Real-time reverse transcription polymerase chain reaction (RT-qPCR)

Total mRNA was extracted from cells in culture by using PureLink® RNA Mini Kit (Life Technologies) and quantified by assessing optical density at 260 and 280 nm via a NanoDrop apparatus (Thermo Scientific). cDNA was synthesized using a mix of random primers, DNTP, Oligo DT12-18 follow by the addition of SuperscriptTM III reverse transcriptase (Life Technologies). Quantitative real-time PCR were carried out using SensiFAST™ SYBR No-ROX (2X, Bioline) on a LightCycler 480 System (Roche Diagnostics) according to the manufacturer's specifications. All qPCR samples were run in duplicate and for each primer pair, a non-template control (NTC) was applied. Specific primers were designed to amplify *cask* (*cask*-F: CCAGGATCAGCATCTTCAC and *cask*-R: TGGCTCTCTGTACTGCATCG and *cask*-F: GTGAAGCCCCACTGTGTTCT and *cask*-R: TTCTGGGGCCATAAAGTGAG), *scn5a* (*snc5a*-F: TATGTCCTCAGCCCCTTCC and *scn5a*-R: GAACACGCAGTTGGTCAGG). All data were normalized to mRNA level of housekeeping genes *polr2a*, *rplp0* and *rpl32* (*polr2a*-F: CGTATCCGCATCATGAACAGTGA and *polr2a*-R: TCATCCATCTTATCCACCACCTCTT; *rplp0*-F: CGACCTGGAAGTCCAACTAC and *rplp0*-R: GTCTGCTCCCACAATGAAG; *rpl32*-F: CCAGAGGCATCGACAACA and *rpl32*-R: GCACTTCCAGCTCCTTGA) using the $2^{-\Delta\Delta CT}$ method.

Electrophysiology

Sodium current was recording in standard whole-cell patch clamp. The perfusion medium for recording I_{Na} was composed, in mmol/L: NaCl 25, CsCl 108.5, HEPES 10, glucose 10, $MgCl_2$ 2.5, $CoCl_2$ 2.5, $CaCl_2$ 0.5 and supplemented with 1 µmol/L of ryanodine, pH adjusted to 7.4 with CsOH. The intrapipette conducting medium was composed, in mmol/L: NaCl 5, $MgCl_2$ 2, $CaCl_2$ 1, EGTA 15, HEPES 10, MgATP 4, CsCl 130, pH adjusted to 7.2 with CsOH. For the current-V_m and activation (m_∞) protocol, currents were elicited by 50ms depolarizing pulses from a holding potential of -120 mV, in 5 or 10 mV increments, between -100 and +60 mV, at a frequency of 0.2 Hz. For the steady-state availability-V_m protocol (h_∞), currents were elicited by a 50ms test pulse to -20 mV following 1s pre-pulses applied in 5 or 10 mv increments, between -140 mV and -20 mV, from a holding potential of -120 mV, at 0.2 Hz.

Statistics

Data were tested for normality using the D'Agostino and Pearson normality test. Statistical analysis was performed using Student's t test or ANOVA followed by post-hoc Student-Newman-Keuls test on raw data. Results are given as means ± SEM and P values of less than 0.05 were considered significant. Legends: ns, not significant; * P<0.05; ** P<0.01 and *** P<0.001.

ACKNOWLEDGMENTS

We thank Dr. Rachel Peat for careful reading of the manuscript and helpful comments. This work was supported by the European Union (EUTRAF-261057; EB and SNH), and by the AFM-Telethon doctoral fellowship (21324; AB). The authors declare no competing financial interests.

AUTHOR CONTRIBUTIONS

Conceptualization: E. Balse. Investigation: A. Beuriot, C.A. Eichel, G. Dilanian, F. Louault, D. Melgari, N. Doisne and E. Balse. Formal analysis: A. Beuriot, A. Coulombe and E. Balse. Funding acquisition: E. Balse and S. Hatem. Supervision: E. Balse. Writing: E. Balse and A. Beuriot.

REFERENCES

1. Zhu J, Shang Y, Zhang M: Mechanistic basis of MAGUK-organized complexes in synaptic development and signalling. Nat Rev Neurosci 2016; 17:209–223.
2. Funke L, Dakoji S, Bredt DS: Membrane-associated guanylate kinases regulate adhesion and plasticity at cell junctions. Annu Rev Biochem 2005; 74:219–245.
3. Butz S, Okamoto M, Südhof TC: A tripartite protein complex with the potential to couple synaptic vesicle exocytosis to cell adhesion in brain. Cell 1998; 94:773–782.
4. LaConte LEW, Chavan V, Liang C, et al.: CASK stabilizes neurexin and links it to liprin-α in a neuronal activity-dependent manner. Cell Mol Life Sci CMLS 2016; 73:3599–3621.
5. Alewine C, Kim B-Y, Hegde V, Welling PA: Lin-7 targets the Kir 2.3 channel on the basolateral membrane via a L27 domain interaction with CASK. Am J Physiol Cell Physiol 2007; 293:C1733-1741.
6. Nix SL, Chishti AH, Anderson JM, Walther Z: hCASK and hDlg associate in epithelia, and their src homology 3 and guanylate kinase domains participate in both intramolecular and intermolecular interactions. J Biol Chem 2000; 275:41192–41200.
7. Maximov A, Sudhof TC, Bezprozvanny I: Association of neuronal calcium channels with modular adaptor proteins. J Biol Chem 1999; 274:24453–24456.
8. Biederer T, Sudhof TC: CASK and protein 4.1 support F-actin nucleation on neurexins. J Biol Chem 2001; 276:47869–47876.
9. Chao H-W, Hong C-J, Huang T-N, Lin Y-L, Hsueh Y-P: SUMOylation of the MAGUK protein CASK regulates dendritic spinogenesis. J Cell Biol 2008; 182:141–155.
10. Hsueh YP, Wang TF, Yang FC, Sheng M: Nuclear translocation and transcription regulation by the membrane-associated guanylate kinase CASK/LIN-2. Nature 2000; 404:298–302.
11. Wang GS, Hong CJ, Yen TY, et al.: Transcriptional modification by a CASK-interacting nucleosome assembly protein. Neuron 2004; 42:113–128.
12. Ojeh N, Pekovic V, Jahoda C, Määttä A: The MAGUK-family protein CASK is targeted to nuclei of the basal epidermis and controls keratinocyte proliferation. J Cell Sci 2008; 121:2705–2717.
13. Zhang Y, Luan Z, Liu A, Hu G: The scaffolding protein CASK mediates the interaction between rabphilin3a and beta-neurexins. FEBS Lett 2001; 497:99–102.
14. Eichel CA, Beuriot A, Chevalier M, et al.: Lateral Membrane-Specific MAGUK CASK Down-Regulates NaV1.5 Channel in Cardiac Myocytes. Circ Res 2016; 119: 544–556.

15. Borg JP, Lõpez-Figueroa MO, de Taddèo-Borg M, et al.: Molecular analysis of the X11-mLin-2/CASK complex in brain. J Neurosci Off J Soc Neurosci 1999; 19:1307–1316.
16. Wong-Riley MTT, Besharse JC: The kinesin superfamily protein KIF17: one protein with many functions. Biomol Concepts 2012; 3:267–282.
17. Jeyifous O, Waites CL, Specht CG, et al.: SAP97 and CASK mediate sorting of N-Methyl-D-Aspartate Receptors through a novel secretory pathway. Nat Neurosci 2009; 12:1011–1019.
18. Lin EI, Jeyifous O, Green WN: CASK Regulates SAP97 Conformation and Its Interactions with AMPA and NMDA Receptors. J Neurosci 2013; 33:12067–12076.
19. Balse E, Eichel C: The Cardiac Sodium Channel and Its Protein Partners. Handb Exp Pharmacol 2018; 246:73–99.
20. Spach MS: Anisotropy of cardiac tissue: a major determinant of conduction? J Cardiovasc Electrophysiol 1999; 10:887–890.
21. Hanada T, Takeuchi A, Sondarva G, Chishti AH: Protein 4.1-mediated membrane targeting of human discs large in epithelial cells. J Biol Chem 2003; 278:34445–34450.
22. Baines AJ, Lu H-C, Bennett PM: The Protein 4.1 family: hub proteins in animals for organizing membrane proteins. Biochim Biophys Acta 2014; 1838:605–619.
23. Cohen AR, Woods DF, Marfatia SM, Walther Z, Chishti AH, Anderson JM: Human CASK/LIN-2 binds syndecan-2 and protein 4.1 and localizes to the basolateral membrane of epithelial cells. J Cell Biol 1998; 142:129–138.
24. Leonoudakis D, Conti LR, Anderson S, et al.: Protein trafficking and anchoring complexes revealed by proteomic analysis of inward rectifier potassium channel (Kir2.x)-associated proteins. J Biol Chem 2004; 279:22331–22346.
25. Gavillet B, Rougier JS, Domenighetti AA, et al.: Cardiac sodium channel Nav1.5 is regulated by a multiprotein complex composed of syntrophins and dystrophin. Circ Res 2006; 99:407–414.

FIGURE LEGENDS

Figure 1. Validation of CASK adenoviral constructs in cardiomyocytes. (A) Schematic representation of CASK structure, domain-specific deletions, and expected molecular weights including a C-terminal GFP reporter **(B)** Representative western blot showing CASK expression in cultured rat cardiomyocytes transduced with each truncated CASK construct. $CASK^{WT}$ fused to GFP corresponds to a ~140 kDa band. GAPDH served as a loading control. **(C)** RT-qPCR histograms of CASK mRNA expression levels in cardiomyocytes transduced with GFP, $CASK^{WT}$, or $CASK^{\Delta X}$, where $^{\Delta X}$ corresponds to any deletion. CASK mRNA levels in cardiac cells is normalized to endogenous CASK mRNA levels under control condition (GFP). Legend: ns, not significant; *** P<0.001; n=number of individual cell cultures; N=3-7 western blot replicates.

Figure 2. Both L27B and GUK CASK domains are implicated in the downregulation of the cardiac sodium current I_{Na} in cultured cardiomyocytes. (A) Current density-voltage relationships (25 mmol/L $[Na^+]_o$) of I_{Na} obtained from cardiomyocytes transduced with GFP control (black), $CASK^{WT}$ (red), or deleted forms of CASK ($CASK^{\Delta X}$). **(B)** Histograms of I_{Na} current density recorded at -20mV and normalized to GFP control. **(C-D)** Voltage-dependent activation and steady-state inactivation curves from cardiomyocytes transduced with GFP control (black), $CASK^{WT}$ (red), or truncated forms of CASK ($CASK^{\Delta X}$). Legend: ns, not significant; *** P<0.001; n=number of cells, N=3-16 independent cell cultures.

Figure 3. Deleting L27B or GUK CASK domains increases cardiac $Na_V1.5$ channel surface expression. (A) Representatives differential interference contrast (DIC) and Total internal reflection fluorescence microscopy (TIRFm) images of both GFP and $Na_V1.5$ signal

taken from fixed cultured cardiomyocytes transduced with either GFP, $CASK^{WT}$, $CASK^{\Delta L27B}$, or $CASK^{\Delta GUK}$**.** Cells were seeded on TIRF-glass micro-dishes and stained with anti-$Na_V1.5$ antibody Cell boundaries were delineated using DIC images and $Na_V1.5$ EFF was quantified in critical angle in GFP control, $CASK^{WT}$, $CASK^{\Delta L27B}$, and $CASK^{\Delta GUK}$**(B)** Histograms of $Na_V1.5$ evanescent field fluorescence (EFF) intensity in arbitrary units and normalized to GFP control. Legend: ns, not significant; * $P < 0.05$; *** $P < 0.001$; n=number of cells; N=4 independent cell cultures.

Figure 4. CASK interacts with dystrophin through its HOOK domain in cardiomyocytes. **(A)** Representative western blot of dystrophin expression after transduction with either GFP control, $CASK^{WT}$, or $CASK^{\Delta X}$. **(B)** Corresponding histograms showing the expression level of dystrophin normalized to GAPDH in cardiomyocytes transduced with the different adenoviral constructs. Legend: ns, not significant; N=5 independent cell cultures. **(C)** Representative co-immunoprecipitation assays performed on cardiomyocyte lysates after transduction with $CASK^{WT}$ or $CASK^{\Delta X}$ showing the loss of association with dystrophin for the $CASK^{\Delta HOOK}$ construct. N=3 independent cell cultures.

Figure 1

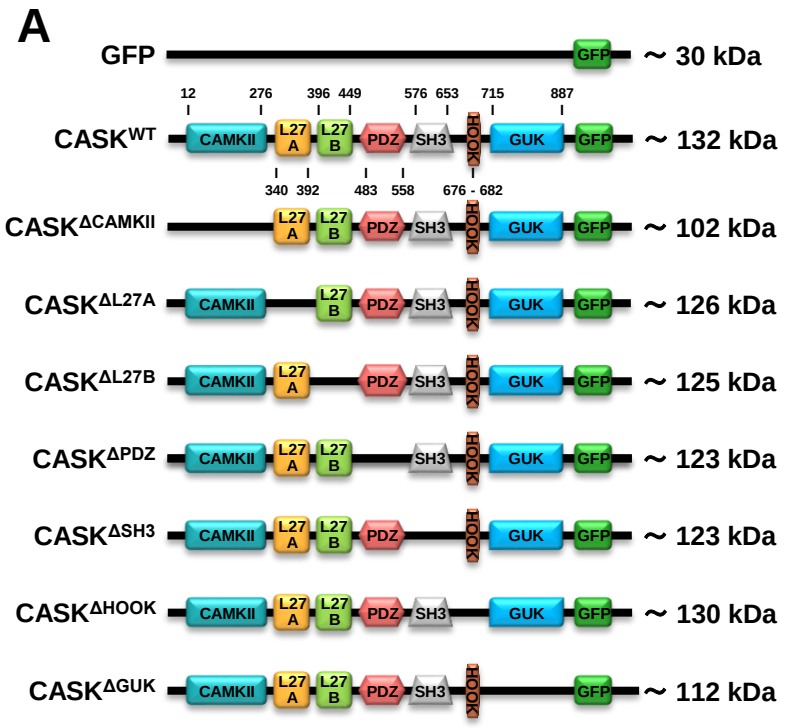
A
GFP
GFP
~ 30 kDa
12
276
396
449
576
653
715
887
CASK^WT
CAMKII
L27 A
L27 B
PDZ
SH3
HOOK
GUK
GFP
~ 132 kDa
340
392
483
558
676 - 682
CASK^ΔCAMKII
~ 102 kDa
CASK^ΔL27A
~ 126 kDa
CASK^ΔL27B
~ 125 kDa
CASK^ΔPDZ
~ 123 kDa
CASK^ΔSH3
~ 123 kDa
CASK^ΔHOOK
~ 130 kDa
CASK^ΔGUK
~ 112 kDa

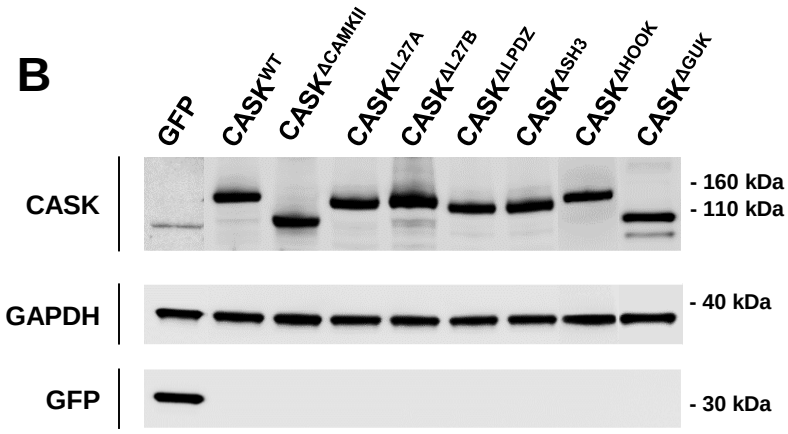
B
GFP
CASK^WT
CASK^ΔCAMKII
CASK^ΔL27A
CASK^ΔL27B
CASK^ΔLPDZ
CASK^ΔSH3
CASK^ΔHOOK
CASK^ΔGUK
CASK
- 160 kDa
- 110 kDa
GAPDH
- 40 kDa
GFP
- 30 kDa

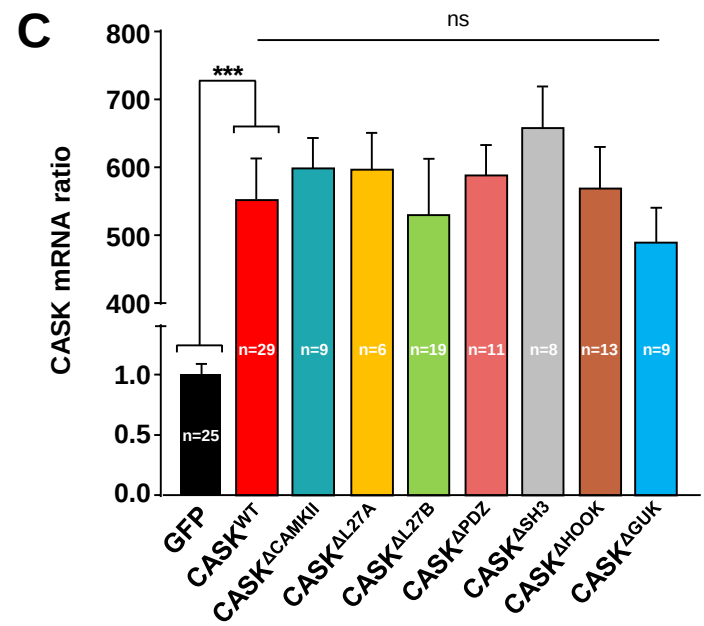
C
ns
***
800
700
600
500
400
1.0
0.5
0.0
CASK mRNA ratio
n=25
n=29
n=9
n=6
n=19
n=11
n=8
n=13
n=9
GFP
CASK^WT
CASK^ΔCAMKII
CASK^ΔL27A
CASK^ΔL27B
CASK^ΔPDZ
CASK^ΔSH3
CASK^ΔHOOK
CASK^ΔGUK

Figure 2

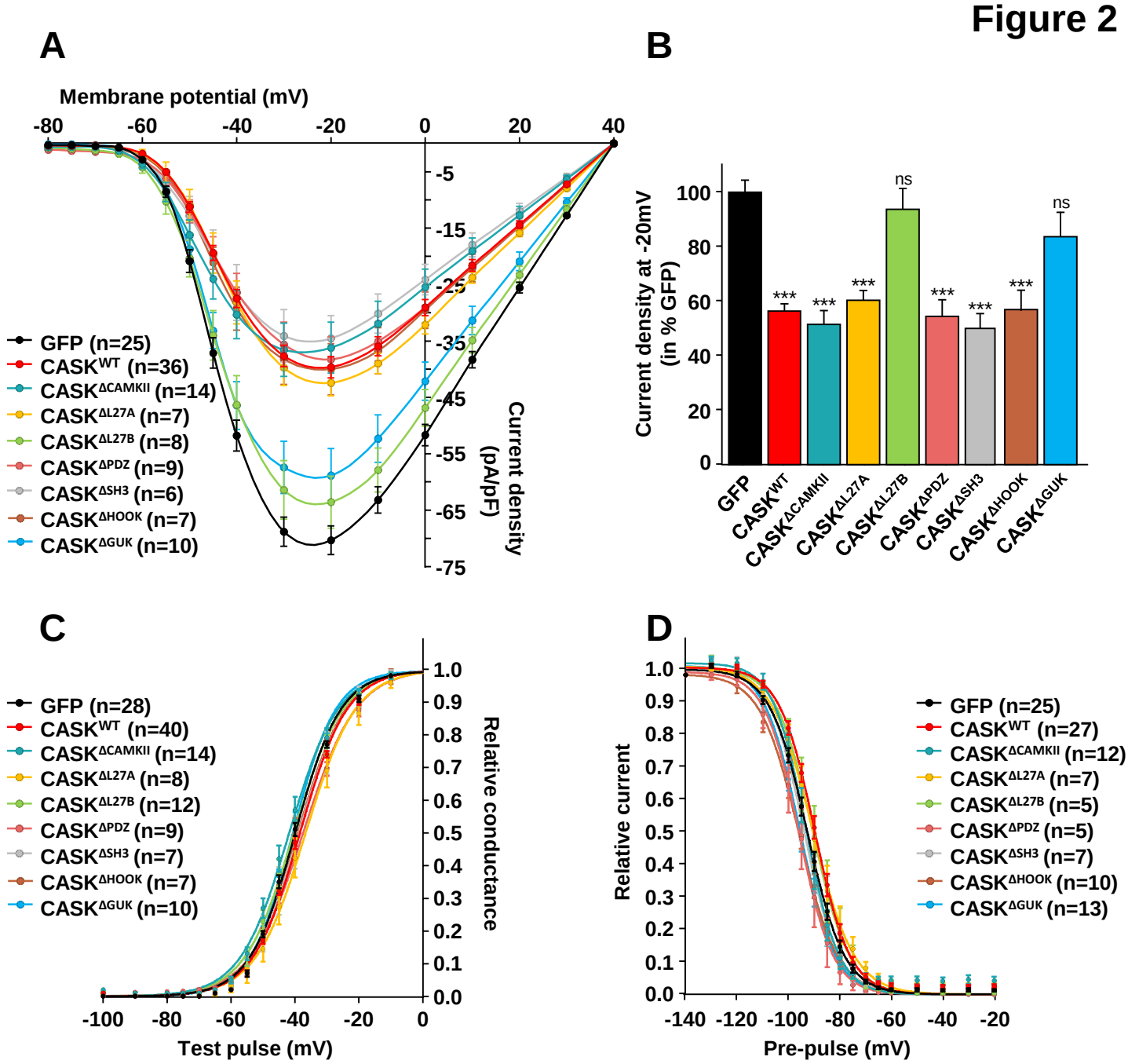
A
Membrane potential (mV)
-80
-60
-40
-20
0
20
40
-5
-15
-25
-35
-45
-55
-65
-75
Current density (pA/pF)
GFP (n=25)
CASK^WT (n=36)
CASK^ΔCAMKII (n=14)
CASK^ΔL27A (n=7)
CASK^ΔL27B (n=8)
CASK^ΔPDZ (n=9)
CASK^ΔSH3 (n=6)
CASK^ΔHOOK (n=7)
CASK^ΔGUK (n=10)
B
Current density at -20mV (in % GFP)
100
80
60
40
20
0
ns
ns
***
***
***
***
***
***
GFP
CASK^WT
CASK^ΔCAMKII
CASK^ΔL27A
CASK^ΔL27B
CASK^ΔPDZ
CASK^ΔSH3
CASK^ΔHOOK
CASK^ΔGUK
C
GFP (n=28)
CASK^WT (n=40)
CASK^ΔCAMKII (n=14)
CASK^ΔL27A (n=8)
CASK^ΔL27B (n=12)
CASK^ΔPDZ (n=9)
CASK^ΔSH3 (n=7)
CASK^ΔHOOK (n=7)
CASK^ΔGUK (n=10)
Relative conductance
1.0
0.9
0.8
0.7
0.6
0.5
0.4
0.3
0.2
0.1
0.0
-100
-80
-60
-40
-20
0
Test pulse (mV)
D
Relative current
1.0
0.9
0.8
0.7
0.6
0.5
0.4
0.3
0.2
0.1
0.0
-140
-120
-100
-80
-60
-40
-20
Pre-pulse (mV)
GFP (n=25)
CASK^WT (n=27)
CASK^ΔCAMKII (n=12)
CASK^ΔL27A (n=7)
CASK^ΔL27B (n=5)
CASK^ΔPDZ (n=5)
CASK^ΔSH3 (n=7)
CASK^ΔHOOK (n=10)
CASK^ΔGUK (n=13)

Figure 3

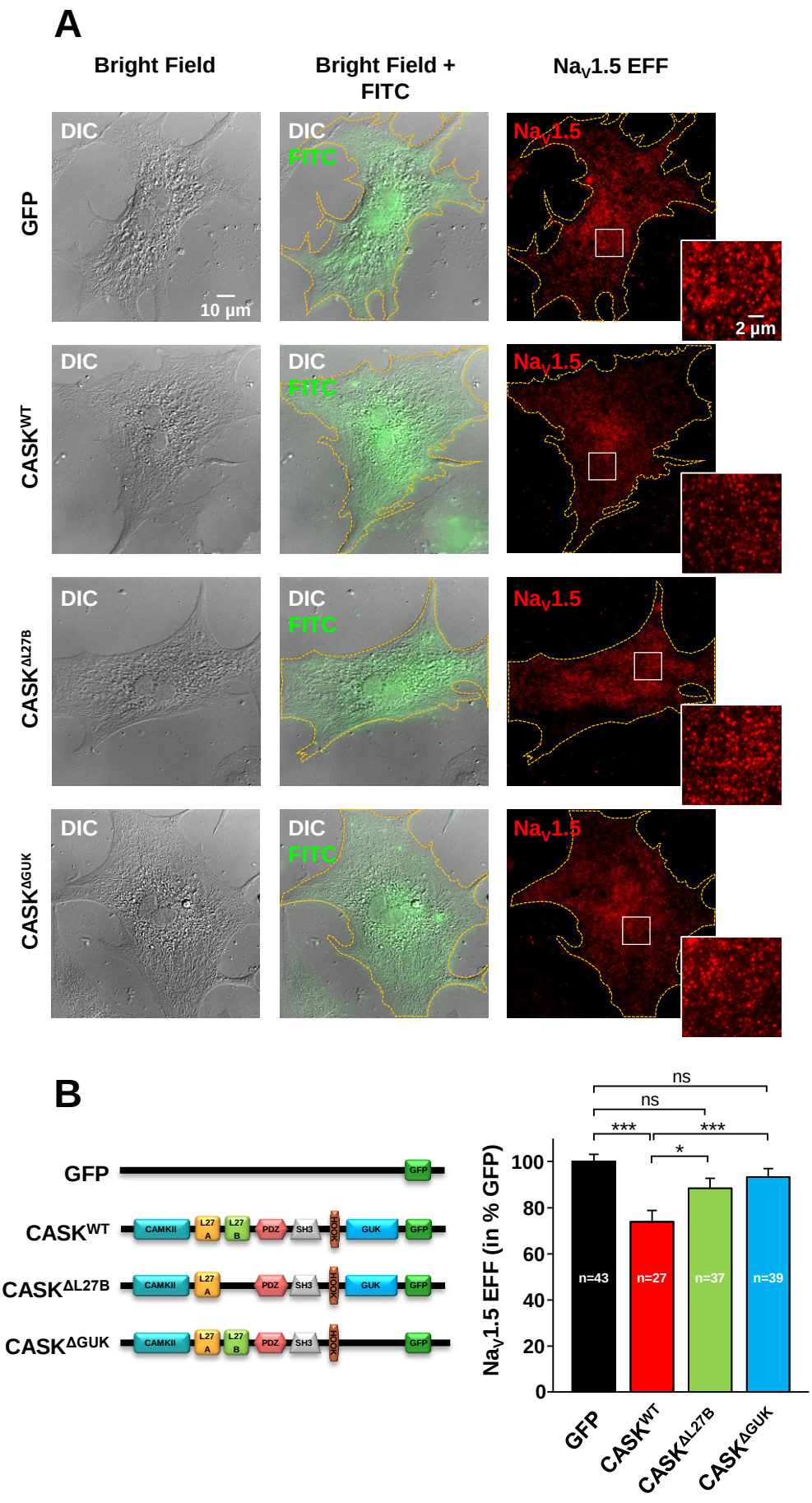
A
Bright Field
Bright Field + FITC
Na$_V$1.5 EFF
GFP
CASK^{WT}
CASK$^{\Delta L27B}$
CASK$^{\Delta GUK}$
DIC
FITC
Na$_V$1.5
10 µm
2 µm
B
GFP
CASK^{WT}
CASK$^{\Delta L27B}$
CASK$^{\Delta GUK}$
CAMKII
L27 A
L27 B
PDZ
SH3
HOOK
GUK
GFP
Na$_V$1.5 EFF (in % GFP)
ns
ns
***
***
*
n=43
n=27
n=37
n=39
0
20
40
60
80
100

Figure 4

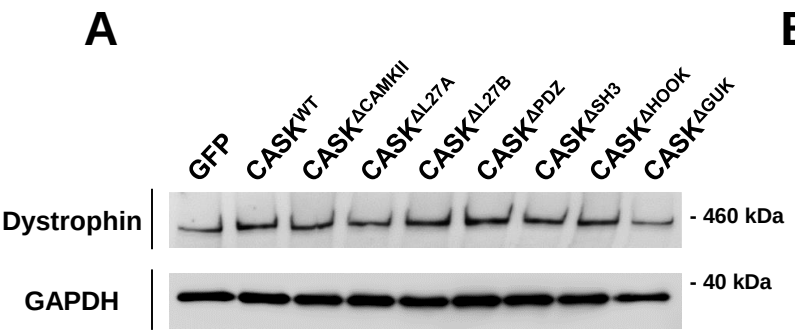
A
GFP
CASK^WT
CASK^ΔCAMKII
CASK^ΔL27A
CASK^ΔL27B
CASK^ΔPDZ
CASK^ΔSH3
CASK^ΔHOOK
CASK^ΔGUK
Dystrophin
GAPDH
- 460 kDa
- 40 kDa

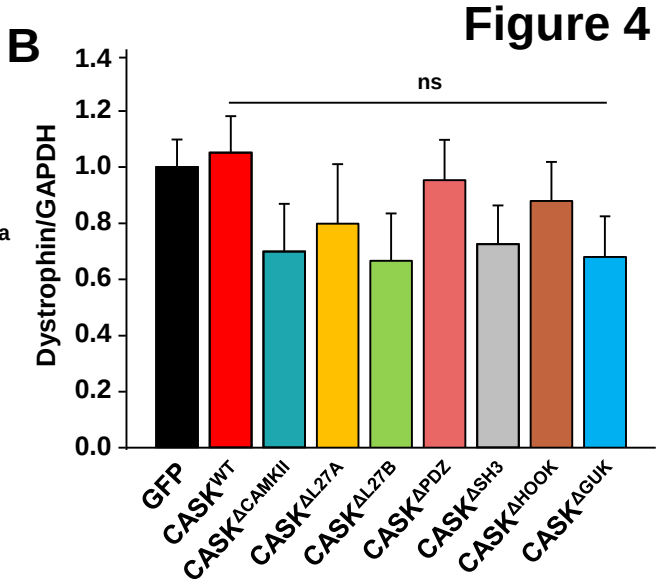
B
ns
Dystrophin/GAPDH
1.4
1.2
1.0
0.8
0.6
0.4
0.2
0.0
GFP
CASK^WT
CASK^ΔCAMKII
CASK^ΔL27A
CASK^ΔL27B
CASK^ΔPDZ
CASK^ΔSH3
CASK^ΔHOOK
CASK^ΔGUK

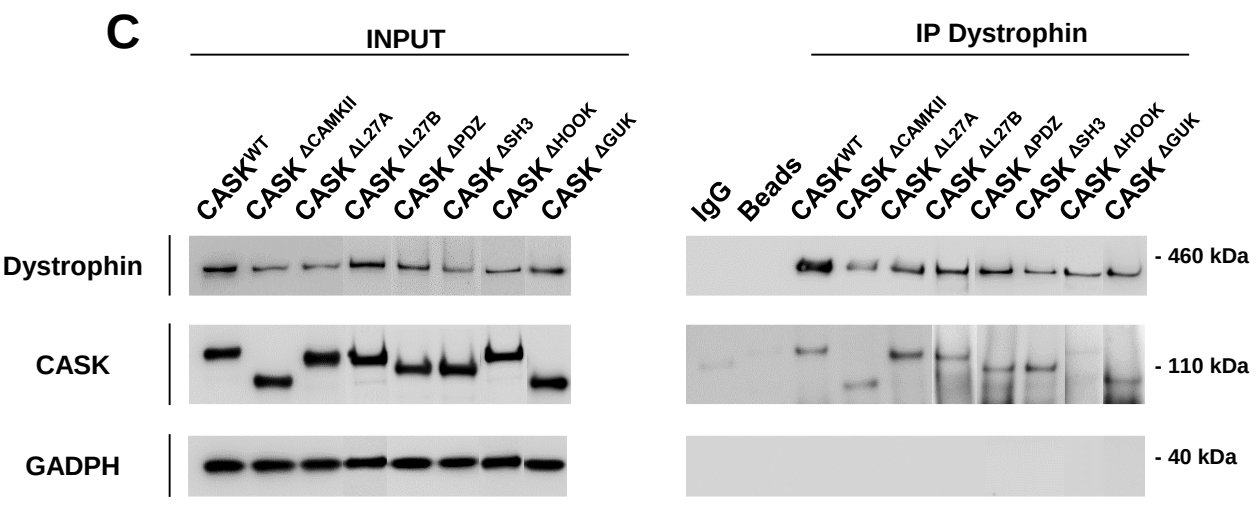
C
INPUT
IP Dystrophin
CASK^WT
CASK ΔCAMKII
CASK ΔL27A
CASK ΔL27B
CASK ΔPDZ
CASK ΔSH3
CASK ΔHOOK
CASK ΔGUK
IgG
Beads
Dystrophin
CASK
GADPH
- 460 kDa
- 110 kDa
- 40 kDa

Supplemental Figure 1

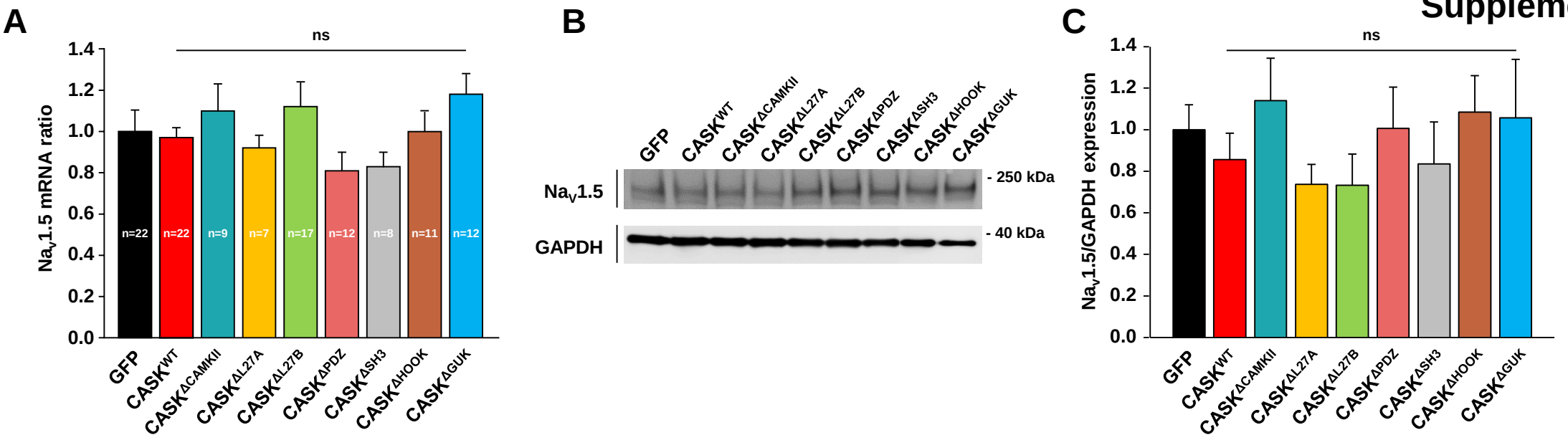

Supplemental Table 1

A

Peak current density at - 20 mV

	Mean raw data (pA/pF)	Current density (% from GFP)	Cell capacitance (pF)
GFP	- 70.4 ± 2.9 (n=25)	100 ± 4.1 (n=25)	53.1 ± 2.4 (n=25)
CASK^{WT}	- 39.6 ± 1.9 (n=36) ***	56.3 ± 2.7 (n=36) ***	48.8 ± 2.4 (n=36) ns
CASK$^{\Delta CAMKII}$	- 36.2 ± 3.7 (n=14) ***	51.4 ± 5.2 (n=14) ***	47.6 ± 2.5 (n=14) ns
CASK$^{\Delta L27A}$	- 42.4 ± 2.5 (n=7) ***	60.3 ± 3.5 (n=7) ***	46.0 ± 3.4 (n=7) ns
CASK$^{\Delta L27B}$	- 65.9 ± 5.3 (n=8) ns	93.7 ± 7.6 (n=8) ns	54.5 ± 6.0 (n=8) ns
CASK$^{\Delta PDZ}$	- 38.3 ± 4.3 (n=9) ***	54.4 ± 6.0 (n=9) ***	54.2 ± 5.9 (n=9) ns
CASK$^{\Delta SH3}$	- 34.6 ± 4.4 (n=6) ***	49.1 ± 6.3 (n=6) ***	44.5 ± 3.8 (n=6) ns
CASK$^{\Delta HOOK}$	- 40.0 ± 4.9 (n=7) ***	56.9 ± 7.0 (n=7) ***	49.2 ± 6.5 (n=7) ns
CASK$^{\Delta GUK}$	- 58.9 ± 6.2 (n=10) ns	83.7 ± 8.9 (n=10) ns	53.5 ± 3.5 (n=10) ns

B

Activation properties

	Membrane potential at half activation $V_{0.5}$ (mV)	Slope factor k (mV)
GFP	-39.9 ± 0.7 (n=28)	6.8 ± 0.2 (n=28)
CASK^{WT}	-38.4 ± 0.5 (n=40) ns	7.2 ± 0.1 (n=40) ns
CASK$^{\Delta CAMKII}$	-41.0 ± 0.3 (n=14) ns	7.4 ± 0.3 (n=14) ns
CASK$^{\Delta L27A}$	-36.5 ± 2.2 (n=8) ns	7.3 ± 0.3 (n=8) ns
CASK$^{\Delta L27B}$	-40.4 ± 1.4 (n=12) ns	7.5 ± 0.3 (n=12) ns
CASK$^{\Delta PDZ}$	-37.4 ± 0.2 (n=9) ns	8.3 ± 0.9 (n=9) **
CASK$^{\Delta SH3}$	-38.7 ± 2.6 (n=7) ns	6.8 ± 0.2 (n=7) ns
CASK$^{\Delta HOOK}$	-39.4 ± 1.5 (n=7) ns	7.39 ± 0.5 (n=7) ns
CASK$^{\Delta GUK}$	-40.7 ± 0.5 (n=10) ns	6.7 ± 0.2 (n=10) ns

C

Inactivation properties

	Membrane potential at half inactivation $V_{0.5}$ (mV)	Slope factor k (mV)
GFP	-92.6 ± 0.8 (n=25)	-6.8 ± 0.2 (n=25)
CASK^{WT}	-89.6 ± 0.9 (n=27) ns	-6.2 ± 0.2 (n=27) ns
CASK$^{\Delta CAMKII}$	-93.2 ± 1.5 (n=12) ns	-5.9 ± 0.4 (n=12) ns
CASK$^{\Delta L27A}$	-90.0 ± 2.1 (n=12) ns	-6.3 ± 0.2 (n=12) ns
CASK$^{\Delta L27B}$	-89.7 ± 3.2 (n=5) ns	-6.6 ± 0.4 (n=5) ns
CASK$^{\Delta PDZ}$	-95.7 ± 2.7 (n=5) ns	-6.0 ± 0.3 (n=5) ns
CASK$^{\Delta SH3}$	-92.8 ± 3.0 (n=7) ns	-6.0 ± 0.5 (n=7) ns
CASK$^{\Delta HOOK}$	-95.7 ± 1.2 (n=10) ns	-7.5 ± 0.4 (n=10) ns
CASK$^{\Delta GUK}$	-95.5 ± 1.2 (n=13) ns	-6.5 ± 0.2 (n=13) ns